THE GERONTOLOGICAL SOCIETY OF AMERICA®

*Journals of Gerontology: Biological Sciences*
cite as: *J Gerontol A Biol Sci Med Sci*, 2021, Vol. XX, No. XX, 1–8
https://doi.org/10.1093/gerona/glab363
Advance Access publication December 6, 2021

OXFORD



Original Article

# Supercomplex Organization of the Electron Transfer System in Marine Bivalves, a Model of Extreme Longevity

**Enrique Rodríguez, PhD,[1,3] Amanda Radke, PhD,[2] Tory M. Hagen, PhD,[2] and Pierre U. Blier, PhD[1,*]**

[1]Département de Biologie, Université du Québec, Rimouski, Québec, Canada. [2]Department of Biochemistry and Biophysics and the Linus Pauling Institute, Oregon State University, Corvallis, Oregon, USA. [3]Present address: Research Department of Genetics, Evolution and Environment, University College London, London, UK.

*Address correspondence to: Pierre U. Blier, PhD, Département de Biologie, Université du Québec, 300 des Ursulines, Rimouski, QC G5L 3A1, Canada. E-mail: pierre_blier@uqar.ca

Received: May 4, 2021; Editorial Decision Date: November 3, 2021

**Decision Editor:** Rozalyn M. Anderson , PhD, FGSA

## Abstract

The mitochondrial oxidative stress theory of aging suggests that the organelle's decay contributes to the aging phenotype *via* exacerbated oxidative stress, loss of organ coordination and energetics, cellular integrity, and activity of the mitochondrial electron transfer system (ETS). Recent advances in understanding the structure of the ETS show that the enzymatic complexes responsible for oxidative phosphorylation are arranged in supramolecular structures called supercomplexes that lose organization during aging. Their exact role and universality among organisms are still under debate. Here, we take advantage of marine bivalves as an aging model to compare the structure of the ETS among species ranging from 28 to 507 years in maximal life span. Our results show that regardless of life span, the bivalve ETS is arrayed as a set of supercomplexes. However, bivalve species display varying degrees of ETS supramolecular organization with the highest supercomplex structures found in *Arctica islandica*, the longest-lived of the bivalve species under study. We discuss this comparative model in light of differences in the nature and stoichiometry of these complexes and highlight the potential link between the complexity of these superstructures and longer life spans.

**Keywords:** Electron transfer system, Invertebrate, Mitochondria, Supercomplex

Mitochondrial dysfunction is postulated to be a key factor in the aging phenotype and the onset of age-related diseases (1). Indeed, mounting evidence from longitudinal and comparative studies points toward a progressive loss of mitochondrial function, linked to the activities of the electron transfer system (ETS) complexes, and the management of reactive oxygen species (ROS) production, in line with the mitochondrial oxidative stress theory of aging (MOSTA, reviewed in Blier and colleagues (2)). Mitochondrial morphology is intimately linked to mitochondrial function (3), and loss of membrane architecture is observed at increasing age (4). In this light, the basic understanding of the physical organization of the enzymatic components in the mitochondrial inner membrane has evolved.

The ETS consists mainly of 4 multisubunit complexes: NADH:ubiquinone oxidoreductase (complex I), succinate dehydrogenase (complex II), coenzyme Q—cytochrome c oxidoreductase III (complex III), the terminal electron acceptor enzyme, cytochrome *c* oxidase (complex IV), plus an ancillary electron transfer flavoprotein complex that augments electron flow into complex III. ETS complexes were first proposed to be assembled into polymeric-protein assemblies within the inner mitochondrial membrane in Chance and William's pioneering studies (5). Later, purification and reconstitution of single enzymatic complexes and kinetic studies led to the proposal of a random diffusion (or fluid) model of electron transfer, where the complexes move randomly and independently within the inner mitochondrial membrane, with electrons flowing between them through mobile carriers coenzyme Q and cytochrome c (for a review see Lenaz and Genova (6)).

Although the fluidity model dominated the mitochondrial field for decades, more recent observations using new kinetic and electrophoretic analysis suggest a different organizational model where a supramolecular organization of the ETS predominates in vivo: the supercomplex (SC). Schägger and Pfeiffer (7) first isolated

and resolved these high-molecular-weight structures composed of varying stoichiometries of complexes I, III, and IV using blue native polyacrylamide gel electrophoresis (BN-PAGE). Initially dismissed as artifacts of the solubilization method, SC assemblies have now been thoroughly demonstrated to occur in vivo, to be fully functional entities, and have been imaged to considerable precision (3). A prime example is the so-called respirasome, an SC ($I_1III_2IV_1$) containing all the redox enzymes required for electron transfer from NADH to molecular oxygen. Other recurring SC assemblies are SC $I_1III_2$ and SC $III_2IV_2$. Very few studies report the presence of complex II-containing SCs and hence its participation in these supramolecular assemblies is unlikely (8).

Preliminary functional hints to the existence of SC came from metabolic flux control analyses, the measurement of the control exerted by individual enzymes on pathways (6). The model of a respiratory chain based on random diffusion of complexes implies different levels of rate control by enzymes, each one controlling the pathway to a certain extent. In contrast, the model based on SC assembly implies electron channeling between complexes and thus, a metabolic pathway behaving as a single component, where inhibition of any component would exert the same flux control. Hence, the sum of all the control coefficients is predicted to be superior to 1, as found by Bianchi et al. (9), who demonstrated a functional association between complexes I and III.

SCs have been proposed to play a role in the management of electron flux and substrate channeling (10) as well as regulate the rate of ROS generation (11). Substrate channeling allows the passing of an intermediate metabolite from one enzyme directly to the other, without release into the substrate pool (9). This bypasses enzyme competition for the substrate, facilitating the reaction. However, there appears to be no confining structure for ubiquinol or cytochrome *c* molecules to guide them to their respective binding sites, and the substrates seem to be freely moving despite the fact that the active sites are in close proximity to each other, in sharp contrast with the typical enzymes that channel substrates (12). The grounds for substrate channeling by SCs have therefore been fiercely debated (13). Nonetheless, a recent cryo-EM resolution of respirasomes and megacomplexes appears to show a more constraining structural conformation of SCs, reviving the idea of substrate channeling as a primary function of SCs (3). Such a structural organization could be beneficial by enhancing electron transfer and limiting reverse electron flow, thus avoiding excessive ROS production at the sensitive ubiquinol-oxidizing site $Q_O$. This could hence be advantageous in the context of oxidative stress management. Some hints at a relationship between the supramolecular structures and the rate of aging have emerged: Most notably, there is increasing evidence for an age-related decline in SC integrity in rat hearts (14). Whether the robustness of these supramolecular assemblies is linked to age-associated decline in organ function or life-span divergences remains unknown (2).

The presence of SC appears not to be universal, and before the relationship between their structure and life-span divergences is scrutinized, their presence in various species needs to be assessed. So far, they have been discovered in a number of organisms: from yeast and fungi to plants, vertebrates, and invertebrates (15). They are however notably absent in *Escherichia coli* where different complexes do not colocalize (16), suggesting an evolutionary adaptation to SC assembly and maintenance. For *Drosophila melanogaster*, one study reported that the ETS complexes were tightly packed but were not arrayed in SC assemblies (17); however, a previous study in flies displaying dysfunctional ATP synthase contradicts these results (18). Thus, it is currently not clear as to how SCs may be linked to age-related mitochondrial dysfunction. Before assessing the aforementioned potential relationship between SC structure and life span, the universality of these structures, and in particular their presence in animal models of longevity, must be assessed.

Various studies on mitochondrial structure and function in marine bivalves, peculiar invertebrate models of longevity, have recently given support to the MOSTA. Among the species compared is the longest-lived noncolonial metazoan, the ocean quahog *Arctica islandica*, which has a maximum reported longevity (MRL) of 507 years in the North Atlantic (19). This is strikingly higher than the MRLs of 3 closely related and similar-sized species: *Mya arenaria* (28 years), *Spisula solidissima* (37 years), and *Mercenaria mercenaria* (106 years (2)). The mitochondrial parameters that may permit the ocean quahog to reach its exceptional longevity include more peroxidation-resistant mitochondrial membranes and lower rates of ROS production (measured as $H_2O_2$ efflux) than other bivalves, despite similar capacities for oxidative phosphorylation (OXPHOS (20,21)). Moreover, we recently reported that the sum of each ETS enzymes' control coefficients in these 4 bivalve species exceeds unity (22), hinting at the presence of SCs (9). Should there be evidence supporting the link between SC structure and life span, it would be revealed in the longest-lived animal known to science. However, we know of no study that has assessed whether the ETS of bivalve mitochondria is arrayed as SCs and, if so, whether SC complexities relate to differences in longevity between species. The objective of the present work was to qualitatively decipher the architecture of the ETS and their organization in species of short- to long-lived bivalves. We show that bivalve ETS, regardless of species, is indeed arrayed in SC assemblies; however, there are distinct differences between species. Our results therefore lay the foundation for a more detailed analysis of SCs in relation to MOSTA and species life span.

## Method

### Bivalve Collection and Mitochondrial Isolation

Bivalve species were either sampled (*Mya arenaria*, *Mercenaria mercenaria*) at low tide, collected by professional divers (*S. solidissima*, *A. islandica* from the Magdalen Islands), or by trawling (*A. islandica* from the Gulf of Maine). Individuals were maintained in flow-through tanks at 8°C for at least a month before the experiments, and shell length was recorded after tissue extraction to estimate individual age. All individuals used were in their adult phase of life and were estimated to be at or close to what constituted their middle age, as measured in our previous studies (21). Mitochondrial isolation was carried out as described (20), except with a modified mitochondrial isolation buffer (23) in which KCl was replaced with NaCl to avoid Coomassie dye precipitation caused by potassium ion (24). The replacement of KCl by NaCl was assessed in a previous study and yielded fully functional mitochondria (22). Approximately 4 g of mantle were pooled from 2 to 4 individuals to ensure a sufficient amount of tissue to obtain an adequate mitochondrial pellet and rinsed in the isolation buffer (400 mM Sucrose, 70 mM HEPES, 50 mM NaCl, 6 mM EGTA, 3 mM EDTA, 10 mg/mL aprotinin, 1% bovine serum albumin [BSA]), minced and homogenized using a glass–Teflon potter on ice. The homogenate was centrifuged at 4°C twice at 1 250 *g* for 10 minutes, discarding the cellular debris fraction and keeping the supernatant. The latter was then centrifuged at 10 500 *g*, and the resulting mitochondrial pellet was resuspended with a 0.5% BSA isolation buffer, centrifuged another time, and resuspended in about 500 µL of buffer. Protein

concentration was immediately determined using the Biuret method, and mitochondrial isolates were divided into 500 µg fractions, freeze-dried in liquid nitrogen, and stored at −80°C until BN-PAGE analysis.

The respiratory function of the remaining mitochondrial isolate was assessed for each sample through high-resolution respirometry at 10°C using an Oxygraph-2K (Oroboros Instruments, Innsbruck, Austria). We assessed the integrity of the outer mitochondrial membrane by the addition of cytochrome *c* (10 µM) during state 3 respiration fueled by substrates glutamate (25 mM) and malate (2 mM) with saturating adenosine diphosphate (5 mM). The activity of cytochrome oxidase (CIV) was also assessed by adding electron donor N'-tetramethyl-p-phenylenediamine (TMPD) (0.5 mM) and ascorbate (2 mM) to avoid the autooxidation of TMPD (22).

### Blue Native PAGE

We performed BN-PAGE on isolated mitochondria by adapting the protocols from Gómez et al, (14) and Witting et al. (24). Frozen mantle mitochondria (175 µg) were slowly thawed on ice and centrifuged at 10 000 *g* for 10 minutes at 4°C. The supernatant was discarded, and the pellet was resuspended in a solubilization buffer (750 mM 6-aminohexanoic acid, 50 mM Bis-Tris, 0.5 mM EDTA disodium salt, pH 7.0). To solubilize mitochondrial membranes and verify that individual ETS complexes could be obtained, *n*-dodecyl-β-D-maltoside (DDM) was used at a 2:1 (w/w) detergent-to-protein ratio in preliminary gels. In gels assessing the presence of SCs, a 20% (w/v) solution of digitonin was added at an empirically determined detergent-to-protein ratio of 8:1 (w/w). After 1-hour of incubation on ice, samples were centrifuged for 35 minutes at 21 100 *g* at 4°C, and the resulting supernatant was transferred to a new Eppendorf tube. A 5% Coomassie G-250 solution was added to a detergent-to-dye ratio of 8:1 (w/w), after which the samples (25 µL) were loaded on NativePAGE 3%–12% Bis-Tris Protein Gels (Thermo Fischer Scientific, Ottawa, Canada). Samples were run in a cathode buffer (50 mM Tricine, 15 mM Bis-Tris, pH 7.0) with 0.02% Coomassie G-250 for 1 hour at 55 V, then voltage was increased to 120 V for another 1 hour. The cathode buffer was replaced by a clear-cathode buffer with 0.002% Coomassie, and samples were run for another 3 hours at 120 V. The apparatus was kept in an ice bath to avoid distortion of lanes. After electrophoresis, gels were destained with water. In-gel activity assays were then performed, or gels were stained using Bio-Safe Coomassie G-250 Stain and imaged with a Bio-Rad ChemiDoc MP system.

### In-Gel Activity Assays

Assays were run according to the protocol devised by Nijtmans and Henderson (25). Gels were preincubated in 5 mM Tris-HCl (pH 7.4) for 15 minutes. Complex I activity was assayed by adding 0.1 mg/mL β-NADH and 2.5 mg/mL p-nitroblue tetrazolium chloride (NBT) and incubating for 10 minutes at room temperature. For complex II, 0.2 mM phenazine methosulfate, 84 mM succinic acid, 50 mM NBT, 10 mM potassium chloride, and 4.5 mM EDTA were added and the gel was incubated at room temperature for 15 minutes. In the complex IV assay, 20 mg 3,3′-diaminobenzidine, 20 mg cytochrome *c*, and 480 units catalase were added, and the gel was incubated for 3 hours at 37°C.

### Gel Band Extraction and Mass Spectrometry Analysis

Gels rinsed with deionized water were used for band extraction and subsequent analysis by mass spectrometry (MS). Gel strips of 2 mm × 5 mm were carefully cut so that cross-band contamination was avoided. The strips were washed with water and destained twice with methanol in 50 mM ammonium bicarbonate ($NH_4HCO_3$). Samples were dehydrated with acetonitrile, then dried in a Speed Vac centrifuge, and rehydrated in 25 mM dithiothreitol, after which they were incubated for 20 minutes at 56°C. After incubation, the supernatant was discarded, and the samples were incubated in the dark at room temperature with 55 mM freshly prepared iodoacetamide. Then, the supernatant was discarded, the samples rinsed twice with water and the dehydration process with acetonitrile was repeated once more. After centrifuging in the Speed Vac, samples were this time rehydrated with a 12 ng/mL Trypsin Gold, MS grade solution in ProteaseMAX (Promega, Madison, WI) surfactant and incubated at 50°C for 1 hour. Tubes were centrifuged at 16 000 *g* for 10 minutes, and the extracted peptides were transferred to a new tube where a 0.5% solution of trifluoroacetic acid was added to inactivate trypsin. Samples were stored at −80°C until MS analysis was performed. They were analyzed by the Oregon State University Mass Spectrometry Center in an Orbitrap Fusion Lumos Tribrid Mass Spectrometer (ThermoFisher).

## Results

### Bivalve Respiratory Function

We assessed the coupling and integrity of each mitochondrial extract by high-resolution respirometry and found the respiratory rates to be in line with previous studies (21,22). Mean NADH-pathway-linked OXPHOS coupling efficiency, calculated as 1-(LEAK state/N-coupled state) (26) in all species, varied between 0.35 (*M. mercenaria*) and 0.55 (*A. islandica* from the Gulf of Maine), reflecting the generally low contribution of this pathway to respiration in marine bivalves. The addition of cytochrome *c* as a measure of outer mitochondrial membrane integrity (quality control test) gave mean increases of coupled N-pathway respiration ranging from 0.49% to 11.33% (often with no increase), hence below the 15% threshold that indicates no substantial damage to mitochondria (21). Complex IV activity varied among species, with *M. mercenaria* showing the highest activity (106.42 ± 42.73 pmol$O_2$/s/mg), *A. islandica* with varying activity depending on the population (Magdalen Islands: 23.04 ± 1.95, Gulf of Maine: 76.70 ± 13.43 pmol$O_2$/s/mg), while both *M. arenaria* and *S. solidissima* showed the lowest activities (12.45 ± 1.72 and 12.50 ± 4.06 pmol$O_2$/s/mg, respectively). See Table 1 for detailed results and the age of the individuals included in this study, estimated from shell length.

### Blue Native PAGE on Mitochondrial Extracts Reveals SC Assemblies

Supplementary Figure 1 shows representative results of the empirical determination of the detergent-to-protein ratio for an optimal BN-PAGE analysis. Different separation patterns are visible from 2:1 to 10:1 digitonin:protein (w/w) ratios for the shortest-lived species *M. arenaria*. This determination was repeated twice for species *M. arenaria* and *A. islandica* in preliminary analyses, and the ratios showing excessive protein smearing and suboptimal bands separation and resolution were deemed unsuitable. The optimal ratio was set at 8:1 digitonin:protein (w/w) and was used to make further species comparisons.

In-gel activity assays for complexes I and IV among our 4 species of interest are shown in Figure 1A. Species are presented from left to right in order of increasing maximum life span and show

**Table 1.** Mitochondrial Respiratory Function Parameters and Integrity of the Outer Mitochondrial Membrane (cytochrome *c* test) in the 3 Marine Bivalve Species Used for Supercomplex Analysis

| Species (*n*) | MRL (years) | Estimated Age (years) | $i_{ADP}$ | Cyt. *c* Test (max. % increase in respiration) | Complex IV Activity (pmol$O_2$/s/mg protein) |
|---|---|---|---|---|---|
| *Mya arenaria* (3) | 28 | 8–10 | 0.44 (±0.19) | 0.76 | 12.45 (±1.72) |
| *Spisula solidissima* (3) | 37 | 10+ | 0.38 (±0.09) | 0.52 | 12.50 (±4.06) |
| *Mercenaria mercenaria* (2) | 106 | 30–40 | 0.35 (±0.14) | 0.49 | 106.42 (±42.73) |
| *Arctica islandica* from the Gulf of Maine (3) | 507 | 50–75 | 0.55 (±0.04) | 11.33 | 76.70 (±13.43) |
| *A. islandica* from the Magdalen Islands (3) | 507 | 140–160 | 0.45 (±0.08) | 6.82 | 23.04 (±1.95) |

*Notes:* $i_{ADP}$ is the OXPHOS coupling efficiency for N-pathway-linked respiration. Maximum reported longevities for the species (MRL) and range of estimated ages based on shell height and length-at-age models (27–31) are also reported. Values for respirometry are ±SEM, except for the cytochrome *c* tests where a maximal increase in respiration is reported.

commonalities and differences in banding patterns. The activity assays demonstrated the existence of active ETS complexes in different assemblies corresponding to a range of molecular weights between 1 236 and 720 kDa. These results are crucial because they demonstrate that the digitonin solubilization conditions did not substantially damage the ETS complexes, and differences in color intensity suggested variations in the amount of complexes in particular bands. The first prominent band below the 1 048 kDa marker appeared common to all species, and the in-gel activity of complex I suggested more presence of this complex in this band. In all of the species examined, the activity assays suggested a colocalization of complexes I and IV within the same band. Complex IV activity was qualitatively more pronounced in *M. arenaria* than in the other 3 species, while *S. solidissima* exhibited very faint bands for both complexes. *M. mercenaria* and *A. islandica* showed more intense complex I activity in the high-molecular-weight bands than the 2 shorter-lived species. Combined together, these elements suggested the existence of SCs in marine bivalves. Because of these results, we further assessed the presence of SCs by MS.

## Patterns of SCs Assemblies and Identification of Proteins by Lumos MS

Figure 1B presents the detailed pattern and composition of mitochondrial ETS SCs evident in the 4 species of bivalves. The highest molecular weight protein bands that were observed in all the bivalve species corresponded to a molecular weight of ~1 MDa. These results strongly supported the in-gel activity data as it suggested the existence of SC assemblies. For ease of analysis, bands are hereafter named S1–S5. In the expanded area presented in Figure 1B, band S1 appeared present in *A. islandica* but less so in other species, while bands S2 and the aforementioned S3 were present in all species. Band S4 and the band presumably containing free complex I (determined from the in-gel activity and position with respect to the marker) were common to all species, but much fainter in *S. solidissima*, a species that showed a strikingly different banding pattern. Band S5 was only apparent in the 2 longest-lived species *A. islandica* and *M. mercenaria*. No differences were found in the banding pattern between the 2 *A. islandica* populations sampled, and the results shown throughout this study are for the Magdalen Islands population.

Results from the MS analysis further revealed which proteins comprised each band (Figure 1B). Band S1 only contained complex I in shorter-lived species (presumably in multiple units), whereas in *M. mercenaria* it contained complexes I, III, and IV, hence forming a respirasome containing all the complexes for electron transfer to molecular oxygen. In *A. islandica*, no complex III was detected, and only complexes I and IV appeared in band S1. Band S2 contained a respirasome (I, III, and IV), as well as complex V in *M. arenaria*. In *S. solidissima* and *M. mercenaria*, only complexes I and IV were detected in this band, while in *A. islandica*, it was composed of I, IV, and V. Band S3 also varied in composition between species, containing complexes I and IV in *M. arenaria*, while only complex I was found in *S. solidissima* and *M. mercenaria*. In *A. islandica* however, this band was similar to S2 but composed of 2 different subunits of complex I (NAD 3 and 5, see figure for details). Composition of band S4 varied from containing complex III (*M. arenaria*) to complex I (*S. solidissima* and *M. mercenaria*) while it was an SC composed of I, IV, and V in *A. islandica*. The band presumed to contain free complex I (see paragraph above) was actually found to be composed of complexes I and IV in all species, except *M. mercenaria* where it also contained complex V. Finally, band S5 only contained

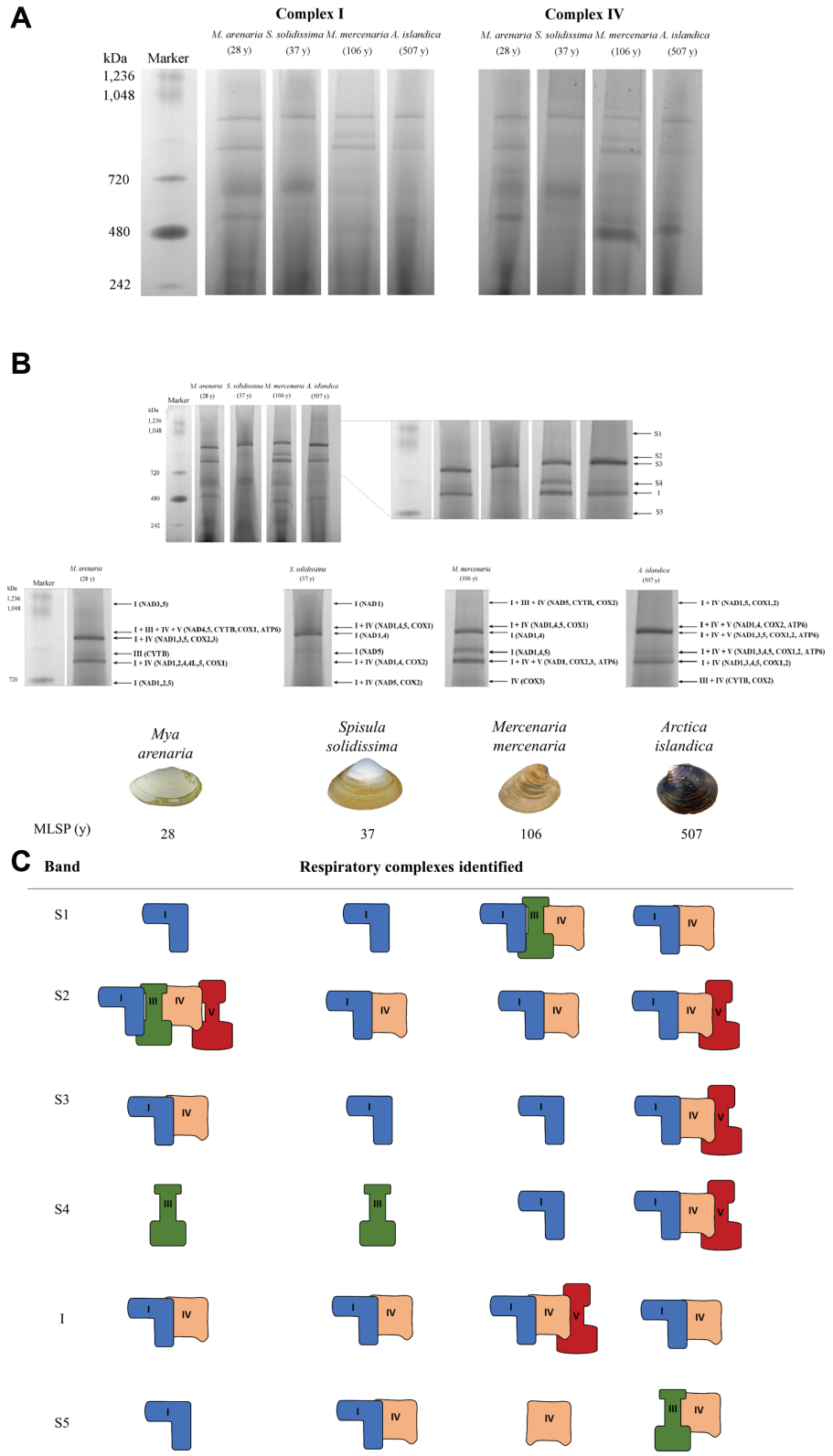


**Figure 1.** (**A**) In-gel activity assays of complexes I and IV in mantle mitochondria of 4 marine bivalves ranked from shortest- to longest-lived and separated by blue native polyacrylamide gel electrophoresis (BN-PAGE). Mitochondria were solubilized with a digitonin-to-protein ratio of 8:1 (w/w), and a NativeMark molecular weight standard was added as a means of estimating molecular weight of the resulting bands. (**B**) Mitochondrial electron transport supercomplexes show different patterns in 4 marine bivalve species with increasing longevities. Mantle mitochondria solubilized with a digitonin-to-protein ratio of 8:1 (w/w), and a NativeMark molecular weight standard separated by BN-PAGE and stained with Coomassie. The blow-up region shows the different SC assembly patterns, and the detailed composition of each resulting band, as obtained by Lumos MS analysis. The genes corresponding to each subunit are shown in parenthesis. (**C**) Graphic depicting the complexes found in each species and the corresponding band.

complex I (*M. arenaria*) or complex IV (*M. mercenaria*), while in *S. solidissima* it was composed of complexes I and IV, and in *A. islandica* contained complexes III and IV, the only such arrangement among all bands across species.

## Discussion

We report for the first time, to our knowledge, evidence for SC organization in marine invertebrates, increasing the generality of these structures among metazoans. Furthermore, we describe differences in the extent and precise nature of SCs in the bivalves under study. Outside of this fundamental contribution to mitochondrial ETS organization in bivalves, we show that there is an apparent increase in SC complexity that correlates with an increased life span. In *A. islandica*, the 6 bands in the high-molecular-weight region contained multiple enzyme complexes, while in all other species, only 3 of those bands had SCs. This long-lived species showed various SCs containing complexes I, IV, and ATP synthase (complex V), rarely encountered in the other 3 species. Interestingly, the respirasome (an SC containing all the complexes for electron transport to molecular oxygen) was found in *M. mercenaria* and *M. arenaria*, but not *A. islandica*. It is also of note that we could not find complex II in our SCs, as generally reported (32). Beyond these general qualitative differences in complexity among species, whether SC integrity in bivalves is associated with individual age as seen in aging rat hearts (14), and whether longer-lived species have more robust structures remains to be meticulously evaluated.

The interactions between enzymatic complexes in SC assemblies are proposed to allow the formation of exclusive electron pathways and minimize ROS production (3). Considering the MOSTA (2), SC assembly is therefore potentially crucial to minimize damage to the mitochondrion. A clear indication of that is the important consequences observed after a loss in the stability of SCs. Lipid peroxidation can disrupt SCs: Maranzana et al. (33) found that dissociation of SC with DDM led to an increase in hydrogen peroxide and superoxide in bovine heart mitochondria and reconstituted liposomes of complexes I and III. When investigating age-related differences in the electron transport system organization of hearts of young and old rats, Gómez et al. (14) found that the levels of individual complexes did not vary. However, they separated and identified the SCs and showed that their levels were diminished between 13% and 25% in old rats versus young individuals, especially for those SCs with higher molecular weight. Overall, this implies that older individuals had more free complexes; and while these might seem as small decrease in SCs, they are actually comparable to those found in pathological studies with important mitochondrial structural and respiratory chain defects, such as Barth or Leigh Syndromes (14). Their results ultimately suggest that there is either an impairment in formation or an increase in the rate of decomposition of SCs in aging heart mitochondria. Aging is therefore accompanied by a decrease in SC association, and an increase in ROS and oxidative damage. If SC stability is key in determining mitochondrial aging phenotype, species differences in MLSP could be related to their capacity to maintain SC integrity.

We previously reported life-span-related differences in control strength among ETS complexes (22), which could explain the proposed link between SC complexity and life span. Indeed, the complex I-linked NADH pathway had no control over respiration in longer-lived species, while the complex IV pathway exerted a strong control, particularly in *A. islandica*. In the current study, we observed the presence of complex IV in all the SC-containing bands extracted from this extremely long-lived species, a unique case among the bivalves herein studied, which could explain its strong control over respiration. This should be investigated further and the analysis be refined to compare activity patterns of in-gel activities among species, as well as quantifying the abundance of protein complexes in the bands, which were not done in this study. We could however appreciate a higher intensity of complex IV banding in *M. arenaria* compared to the other species, which does not reflect its activity as measured by respirometry (Table 1). This could be due to the technical difference between measuring the free activity of the enzyme in the in-gel assay and the measurement in a functional mitochondrial environment, where oxygen consumption with an artificial electron donor is measured.

The current understanding of the nature of SCs has evidenced assemblies of varied composition and important diversity both among and within species, tissues, and cellular type. For example, OXPHOS-dependent rat neurons have more complex I assembled into SCs than glycolysis-reliant astrocytes, which have more free complex I, and produce more ROS (11). Knockdown of a major complex I subunit (NDUFS1) disassembled this enzyme from SCs, impairing electron transfer as shown by the decrease in respiration, and increased ROS production. This is consistent with another study showing that a more efficient assembly of complex I, associated with a lower abundance of free complex I, increased efficiency of substrate utilization, minimized ROS production, and increased longevity in mice liver and brain (34). Anoxia-resistant turtles have been shown to possess SCs that are more stable when exposed to the detergent DDM than those of mammalian models, and this stability was proposed to confer protection against ROS burst upon reoxygenation (35). In a follow-up study (36), the low aerobic capacity and ROS production in anoxic conditions were because of a reduction in substrate oxidation, possibly via the downregulation of ETS complexes activities, rather than to modifications in mitochondrial morphology. Indeed, neither mitochondrial content, morphology (volume density or cristae surface area), nor SC composition or stability changed between warm-acclimated normoxic or cold-acclimated normoxic and anoxic treatments. While exposure to low temperature and anoxia does not change SC distribution, perhaps the important SC robustness previously shown in this species (35) partly explains their tolerance to such conditions and reoxygenation, a feat that could be verified by comparing this tolerant species' SC architecture to other less-tolerant and related species. Given the exceptionally high resistance to low oxygen conditions in *A. islandica* (37) and the differences in the environmental conditions (marine vs coastal and estuarine habitats) faced by the species studied herein, it would be interesting to assess whether the differences in SC assemblies could also be linked to tolerance to oxygen concentration in parallel with longevity.

In conclusion, we demonstrate the existence of SC in marine invertebrates, further proving their ubiquitous nature in animals. The differences in the nature and distribution of SCs among species of varying life span allow us to speculate that if these structures are associated with life span, their specific composition in long-lived species (ie, high complexity and association with complex V) should be a trait promoting extreme longevity.

## Supplementary Material

Supplementary data are available at *The Journals of Gerontology, Series A: Biological Sciences and Medical Sciences* online.

## Funding

This research was supported by an Fonds de recherche du Québec – Nature et technologies (FRQNT) international travel grant to E.R., an Natural Sciences and Engineering Research Council of Canada (NSERC) grant to P.U.B. (RGPIN-2019-05992), and the National Institutes of Health/National Institute on Aging grant to T.M.H. (1R21AG060206-01A1).

## Conflict of Interest

None declared.

## Acknowledgments

The authors would like to acknowledge the help of Judy Butler, Nicholas O. Thomas, and Luis Gómez at the Linus Pauling Institute for their help with the experiments and data interpretation. Stanislau Stanisheuski and Liping Yang (OSU Mass Spectrometry Center) provided invaluable assistance with the MS analysis of the samples. We are also very grateful to Marie-Pier Forest and Dr. Amine Badri of CRBM (Rimouski, Quebec) for their help with image acquisition.

## Data Availability

Original gel images can be found here:

Enrique Rodriguez, Pierre U. Blier, Tory M. Hagen. (2021). Supporting images for the paper: supercomplex organization of the electron transfer system in marine bivalves, a model of extreme longevity. University College London. Dataset. https://doi.org/10.5522/04/17104637.v1

## References

1. Barja G. Towards a unified mechanistic theory of aging. *Exp Gerontol*. 2019;124:110627. doi:10.1016/j.exger.2019.05.016
2. Blier PU, Abele D, Munro D, Degletagne C, Rodriguez E, Hagen T. What modulates animal longevity? Fast and slow aging in bivalves as a model for the study of lifespan. *Semin Cell Dev Biol*. 2017;70:130–140. doi:10.1016/j.semcdb.2017.07.046
3. Guo R, Gu J, Zong S, Wu M, Yang M. Structure and mechanism of mitochondrial electron transport chain. *Biomed J*. 2018;41(1):9–20. doi:10.1016/j.bj.2017.12.001
4. Daum B, Walter A, Horst A, Osiewacz HD, Kühlbrandt W. Age-dependent dissociation of ATP synthase dimers and loss of inner-membrane cristae in mitochondria. *Proc Natl Acad Sci U S A*. 2013;110(38):15301–15306. doi:10.1073/pnas.1305462110
5. Chance B, Williams GR. A method for the localization of sites for oxidative phosphorylation. *Nature*. 1955;176(4475):250–254. doi:10.1038/176250a0
6. Lenaz G, Genova ML. Kinetics of integrated electron transfer in the mitochondrial respiratory chain: random collisions vs. solid state electron channeling. *Am J Physiol Cell Physiol*. 2007;292(4):C1221–C1239. doi:10.1152/ajpcell.00263.2006
7. Schägger H, Pfeiffer K. Supercomplexes in the respiratory chains of yeast and mammalian mitochondria. *EMBO J*. 2000;19(8):1777–1783. doi:10.1093/emboj/19.8.1777
8. Guo R, Zong S, Wu M, Gu J, Yang M. Architecture of human mitochondrial respiratory megacomplex I2III2IV2. *Cell*. 2017;170(6):1247–1257.e12. doi:10.1016/j.cell.2017.07.050
9. Bianchi C, Genova ML, Parenti Castelli G, Lenaz G. The mitochondrial respiratory chain is partially organized in a supercomplex assembly: kinetic evidence using flux control analysis. *J Biol Chem*. 2004;279(35):36562–36569. doi:10.1074/jbc.M405135200
10. Lapuente-Brun E, Moreno-Loshuertos R, Acín-Pérez R, et al. Supercomplex assembly determines electron flux in the mitochondrial electron transport chain. *Science*. 2013;340(6140):1567–1570. doi:10.1126/science.1230381
11. Lopez-Fabuel I, Le Douce J, Logan A, et al. Complex I assembly into supercomplexes determines differential mitochondrial ROS production in neurons and astrocytes. *Proc Natl Acad Sci U S A*. 2016;113(46):13063–13068. doi:10.1073/pnas.1613701113
12. Milenkovic D, Blaza JN, Larsson NG, Hirst J. The enigma of the respiratory chain supercomplex. *Cell Metab*. 2017;25(4):765–776. doi:10.1016/j.cmet.2017.03.009
13. Fedor JG, Hirst J. Mitochondrial supercomplexes do not enhance catalysis by Quinone channeling. *Cell Metab*. 2018;28(3):525–531.e4. doi:10.1016/j.cmet.2018.05.024
14. Gómez LA, Monette JS, Chavez JD, Maier CS, Hagen TM. Supercomplexes of the mitochondrial electron transport chain decline in the aging rat heart. *Arch Biochem Biophys*. 2009;490(1):30–35. doi:10.1016/j.abb.2009.08.002
15. Cogliati S, Calvo E, Loureiro M, et al. Mechanism of super-assembly of respiratory complexes III and IV. *Nature*. 2016;539(7630):579–582. doi:10.1038/nature20157
16. Llorente-Garcia I, Lenn T, Erhardt H, et al. Single-molecule in vivo imaging of bacterial respiratory complexes indicates delocalized oxidative phosphorylation. *Biochim Biophys Acta*. 2014;1837(6):811–824. doi:10.1016/j.bbabio.2014.01.020
17. Shimada S, Oosaki M, Takahashi R, et al. A unique respiratory adaptation in *Drosophila* independent of supercomplex formation. *Biochim Biophys Acta Bioenerg*. 2018;1859(2):154–163. doi:10.1016/j.bbabio.2017.11.007
18. Celotto AM, Chiu WK, Van Voorhies W, Palladino MJ. Modes of metabolic compensation during mitochondrial disease using the *Drosophila* model of ATP6 dysfunction. *PLoS One*. 2011;6(10):e25823. doi:10.1371/journal.pone.0025823
19. Butler PG, Wanamaker AD, Scourse JD, Richardson CA, Reynolds DJ. Variability of marine climate on the North Icelandic Shelf in a 1357-year proxy archive based on growth increments in the bivalve *Arctica islandica*. *Palaeogeogr Palaeoclimatol Palaeoecol*. 2013;373:141–151. doi:10.1016/j.palaeo.2012.01.016
20. Munro D, Blier PU. The extreme longevity of *Arctica islandica* is associated with increased peroxidation resistance in mitochondrial membranes. *Aging Cell*. 2012;11(5):845–855. doi:10.1111/j.1474-9726.2012.00847.x
21. Munro D, Pichaud N, Paquin F, Kemeid V, Blier PU. Low hydrogen peroxide production in mitochondria of the long-lived *Arctica islandica*: underlying mechanisms for slow aging. *Aging Cell*. 2013;12(4):584–592. doi:10.1111/acel.12082
22. Rodríguez E, Hakkou M, Hagen TM, Lemieux H, Blier PU. Divergences in the control of mitochondrial respiration are associated with lifespan variation in marine bivalves. *J Gerontol A Biol Sci Med Sci*. 2020;76(5):796–804. doi:10.1093/gerona/glaa301
23. Moyes CD, Moon TW, Ballantyne JS. Glutamate catabolism in mitochondria from *Mya arenaria* mantle: effects of pH on the role of glutamate dehydrogenase. *J Exp Zool*. 1985;236(3):293–301. doi:10.1002/jez.1402360306
24. Wittig I, Braun HP, Schägger H. Blue native PAGE. *Nat Protoc*. 2006;1(1):418–428. doi:10.1038/nprot.2006.62
25. Nijtmans LG, Henderson NS, Holt IJ. Blue native electrophoresis to study mitochondrial and other protein complexes. *Methods*. 2002;26(4):327–334. doi:10.1016/S1046-2023(02)00038-5
26. Gnaiger E, Group MT. Mitochondrial physiology. *Bioenerg Commun*. 2020;1:44. doi:10.26124/bec:2020-0001.v1
27. Pace SM, Powell EN, Mann R, Long MC, Klinck JM. Development of an age-frequency distribution for ocean quahogs (*Arctica islandica*) on Georges Bank. *J Shellfish Res*. 2017;36(1):41–53. doi:10.2983/035.036.0106
28. Ridgway ID, Richardson CA, Enos E, et al. New species longevity record for the Northern Quahog (=Hard Clam), *Mercenaria mercenaria*. *J Shellfish Res*. 2011;30(1):35–38. doi:10.2983/035.030.0106
29. Giguère M, Brulotte S, Paille N, Fortin J. Mise à jour des connaissances sur la biologie et l'exploitation de la mactre de l'Atlantique (*Spisula*

*solidissima*) aux Îles-de-la-Madeleine. 2005;2587:ix + 32. https://publications.gc.ca/site/eng/9.604056/publication.html

30. Brousseau DJ. Analysis of growth rate in *Mya arenaria* using the Von Bertalanffy equation. *Mar Biol*. 1979;51(3):221–227. doi:10.1007/BF00386801
31. Filippenko D, Naumenko E. Patterns of the growth of soft-shell clam *Mya arenaria* L. (Bivalvia) in shallow water estuaries of the southern Baltic Sea. *Ecohydrol Hydrobiol*. 2014;14(2):157–165. doi:10.1016/j.ecohyd.2014.03.002
32. Jang S, Javadov S. Elucidating the contribution of ETC complexes I and II to the respirasome formation in cardiac mitochondria. *Sci Rep*. 2018;8(1):17732 1–12. doi:10.1038/s41598-018-36040-9
33. Maranzana E, Barbero G, Falasca AI, Lenaz G, Genova ML. Mitochondrial respiratory supercomplex association limits production of reactive oxygen species from complex I. *Antioxid Redox Signal*. 2013;19(13):1469–1480. doi:10.1089/ars.2012.4845
34. Miwa S, Jow H, Baty K, et al. Low abundance of the matrix arm of complex I in mitochondria predicts longevity in mice. *Nat Commun*. 2014;5:1–12. doi:10.1038/ncomms4837
35. Bundgaard A, James AM, Joyce W, Murphy MP, Fago A. Suppression of reactive oxygen species generation in heart mitochondria from anoxic turtles: the role of complex I *S*-nitrosation. *J Exp Biol*. 2018;221(8):jeb174391. doi:10.1242/jeb.174391
36. Bundgaard A, Qvortrup K, Rasmussen LJ, Fago A. Turtles maintain mitochondrial integrity but reduce mitochondrial respiratory capacity in the heart after cold-acclimation and anoxia. *J Exp Biol*. 2019;222(11). doi:10.1242/jeb.200410
37. Strahl J, Brey T, Philipp EE, et al. Physiological responses to self-induced burrowing and metabolic rate depression in the ocean quahog *Arctica islandica*. *J Exp Biol*. 2011;214(Pt 24):4223–4233. doi:10.1242/jeb.055178